First-principles study of the electronic, magnetic and structural properties of ZnO and $Zn_{1-x}Cr_xO$ (x = 0.125, 0.25, 0.375, 0.5) in the room temperature wurtzite structure

Sarajit Biswas*

Department of Physics, Taki Government College, P.O. Taki, North 24 Dist, Parganas 743 429, India

First-principles electronic structure calculations were presented to study the electronic, magnetic and structural properties of pure ZnO and $Zn_{1-x}Cr_xO$ (x = 0.125, 0.25, 0.375, 0.5) in the room temperature (293 K) wurtzite structure. Pure ZnO is found to be a non-magnetic insulator due to perfectly paired electrons in each Zn-3d orbital. This material encounters nonmagnetic insulator to a ferromagnetic half-metal for x = 0.125 and then to a ferromagnetic metal for x = 0.25. The ferromagnetic metallic phase maintains up to x = 0.5. It is revealed in this study that 100% spin polarization is responsible for the half-metallic behaviour of $Zn_{0.875}Cr_{0.125}O$. Nevertheless, partial filling of Cr-$3d_{3z^2-r^2}$ orbital in the spin-up channel together with a minute, but finite contribution of electrons from the Cr-$3d_{xy/z^2-r^2}$ orbitals at E_F for the spin-down channel are together responsible for the metallic behaviour of $Zn_{1-x}Cr_xO$ ($x \geq 0.25$). The ferromagnetism in all the Cr-substituted compounds arises from strong Hund's rule coupling. Eventually, a trivial variation in the Zn–O/Zn–Zn bond distances and ∠Zn–O–Zn bond angles caused by Cr doping is responsible for a minor structural distortion in $Zn_{0.5}Cr_{0.5}O$.

Keywords: Bandgap semiconductor, Cr-doped ZnO, electronic and optical properties, density functional theory, wurtzite ZnO.

NANOSTRUCTURED zinc oxide (ZnO) materials have attracted increasing interest in recent years because of their remarkable properties for electrical and optoelectronics applications. Pure ZnO is an n-type semiconductor material with a hexagonal wurtzite ($P6_3mc$) structure[1] having a wide band gap of 3.36 eV and large excitation energy gap of 60 meV. ZnO has attracted much interest for many years due to excellent performance in blue–ultraviolet (UV) and UV regions[2]. Studies on ZnO-based light emitting diodes (LEDs) and laser diodes (LDs) have made great progress in the last decades[3,4]. Due to excellent chemical and thermal stability, specific electrical and optoelectronic property, and since it is a II–VI semiconductor, ZnO nanomaterials have been extensively used for surface acoustic wave devices[5], photonic crystals[6], photo detectors[7], photo diodes[8], chemical and gas sensors[9], optoelectronic devices[10] and solar cells[11].

The doping in ZnO nanoparticles with the controlled substitution of impurities can change its electrical, optical and structural properties. As a consequence, enormous efforts have been devoted to synthesize doped ZnO nanoparticles with impurities such as Cu, Al, In, Sb, Ga, Fe, Co, Ni, etc. Furthermore, combined doping in ZnO nanomaterials also results in massive changes in electrical, optical and structural properties. The combinational doping of Y and Cd or Mn and Co has been reported[9] to affect the structural and optical properties of ZnO nanomaterials. Cobalt (Co) doping in ZnO nanoparticles reduces its grain size and enhances optical properties by narrowing energy band gap[12]. Indium (In) doping also increases the electrical conductivity of ZnO nanoparticles[13]. Therefore, doping in ZnO nanoparticles is frequently used to modify their structural, electrical, magnetic and photophysical properties. Research on doped ZnO nanocrystals has led to major developments in spintronics, dilute magnetic semiconductors (DMS), optical devices and photocatalysis.

It is well known that Cr is a paramagnetic metal at high temperature and becomes antiferromagnetic below 311 K. The only ferromagnetic metal oxide is CrO_2 with high T_c = 386 K. These properties make Cr a suitable and promising doping element for ZnO nanoparticles. Considering these theoretical predictions, significant results have been devoted to this system by Cr doping. Nevertheless, the experimental results are in conflict with each other. For example, no ferromagnetism (FM) was identified in Cr-doped ZnO films prepared by pulsed laser deposition[14] and combinational laser molecular-beam epitaxy methods[15]. On the other hand, some other studies establish that Cr-doped ZnO films are ferromagnetic at room temperature (RT) when synthesized by laser deposition, magnetron sputtering or a sol–gel method[16].

*e-mail: srisabuj.phys@gmail.com

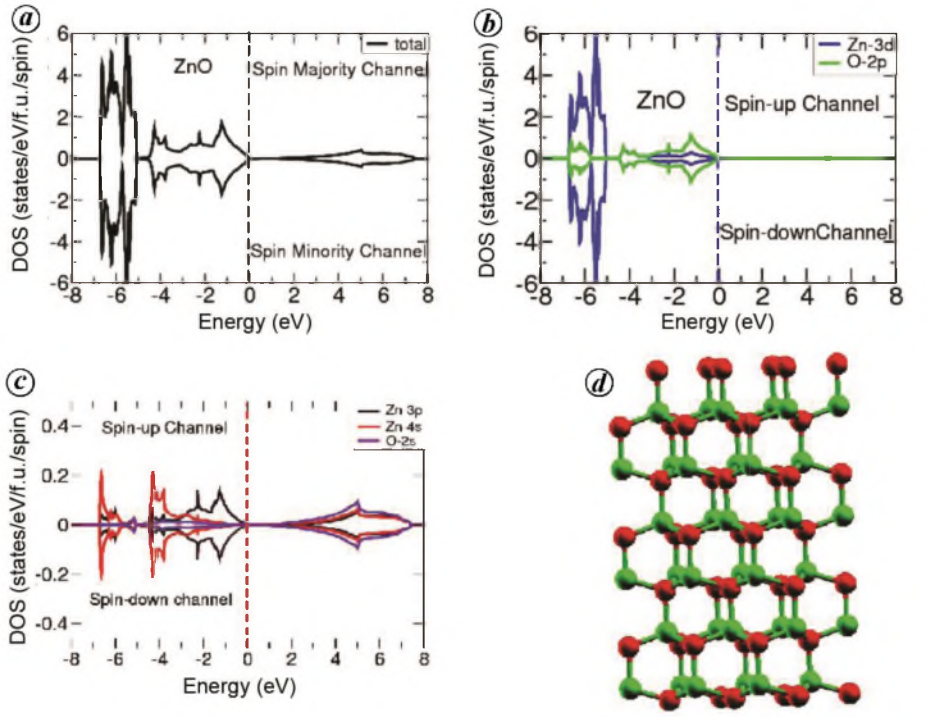

Figure 1. ***a***, Calculated total. ***b***, Zn-3d and O-2p DOS of pure ZnO at 293 K. Band gap observed is 1.90 eV. ***c***, DOS of Zn–3p, 4s and O–2s orbital. The Fermi energy is set to zero. ***d***, The crystal structure of pure ZnO. The green and red spheres correspond to Zn and O atoms respectively.

Although there are many experimental studies on magnetic and non-magnetic doped ZnO films showing room temperature (RT) FM, there is no consensus in the origin of FM ZnO-based materials.

Cr doping in ZnO at RT structure was studied by employing first-principle electronic structure calculations based on density functional theory (DFT) within local density approximation (LDA) formalisms. At 12.5% Cr doping, the system encounters nonmagnetic insulator to a ferromagnetic half-metal. Eventually, this material turns into an FM metal at 25% Cr substitution. Additionally, a slight structural distortion in the $Zn_{1-x}Cr_xO$ compound was observed due to 50% Cr doping. The aim of this study is to investigate the origin of the insulator to half-metal and then half-metal to metal transition in Cr-doped ZnO in the LT phase. Furthermore, the origin of ferromagnetism in the half-metallic or metallic phase is also investigated in this study.

Method of calculations

First-principles electronic structure calculations were carried out to study the electronic, magnetic and structural properties of pure ZnO and Cr-doped $Zn_{1-x}Cr_xO$ (x = 0.125, 0.25. 0.375, 0.5). With this intention, DFT[17,18] implemented in the tight binding linearized-muffin-tin orbitals (TB-LMTO) method within its atomic sphere approximations (ASA)[19,20] was employed using LDA[20,21]. The electronic band structure, densities of states (DOS) and structural properties of both ZnO and $Zn_{1-x}Cr_xO$ were systematically studied. The primitive unit cell of pure ZnO in RT (293 K) hexagonal wurtzite structure (space group $P6_3mc$) consists of two Zn and O sites each. The lattice parameters used are: $a = b = 3.2489$ Å and $c = 5.2049$ Å with Zn located at (1/2, 2/3, 0.3815) and oxygen located at (1/2, 2/3, 0)[1].

Results and discussion

Electronic and magnetic properties of ZnO

The ongoing study was started with the DOS calculations of pure ZnO. The total (black), projected DOS of Zn-3d (blue) and O-2p (green) orbitals are represented in Figure 1 *a* and *b* respectively. It is noticeable from this figure that the DOS for both spin channels are identical. Nevertheless, the system is found insulating in both spin channels. The Cr-3d and O-2p DOS are observed around –6.8 to 0 eV. In this study, the band gap calculated is $E_g \sim 1.9$ eV which is a remarkable improvement over other DFT calculations (0.73–0.75 eV)[22]. Although the calculated band gap is much smaller compared to the experimental value (3.26 eV), this underestimation occurs due to the well-known calculation error of Kohn–Sham DFT for the conduction band. Nonetheless, these results did not affect the accuracy of the comparison of related

Table 1. Calculated total ground state energy (E_T), effective (μ_{eff}), Zn (μ_{Zn}), Cr (μ_{Cr}), O (μ_O)-magnetic moments (μ_B) and conductivity of pure ZnO and $Zn_{1-x}Cr_xO$ (x = 0.125, 0.25, 0.375, 0.5) at 293 K

Compounds	E_T (eV)	μ_{eff} (μ_B)	μ_{Zn} (μ_B)	μ_{Cr} (μ_B)	μ_O (μ_B)	Conductivity
ZnO	–3737.9	0	0	–	0	Insulating
$Zn_{0.875}Cr_{0.125}O$	–3551.7	–4.22	–0.01	–3.97	–0.01	Half–metallic
$Zn_{0.75}Cr_{0.25}O$	–3365.5	–4.03	–0.01	–3.80	–0.02	Metallic
$Zn_{0.625}Cr_{0.375}O$	–3179.4	–3.91	–0.01	–3.60	–0.03	Metallic
$Zn_{0.5}Cr_{0.5}O$	–2993.2	–3.79	–0.01	–3.40	–0.04	Metallic

properties of crystals (e.g. band structure and DOS properties).

The formal valence of Zn in pure ZnO is +2 (Zn^{+2}), i.e. it has ten electrons in its 3d orbitals. It is observable from Figure 1 that the total DOS in the valence band appears predominantly from Zn-3d DOS. All the Zn-3d states are fully occupied by available ten electrons and pushed far below E_F. Due to the presence of hexagonal crystal field, the Zn-3d manifold splits into triply degenerate t_{2g} bands and doubly degenerate e_g bands. The t_{2g} and e_g bands are observed from –6.8 to –5.7 eV and –5.7 to 5.0 eV respectively. The total DOS (TDOS) of Zn-3d and O-2p bands at E_F are also calculated (Table 1). It is found in the TDOS calculations that the occupancy of Zn-3d bands for both spin species is almost equal (~5.0 states/eV/f.u. (formula unit)/spin). Therefore, two species of electrons (up- and down-spin) occupy each of the Zn-3d states in opposite direction resulting in nonmagnetic nature of pure ZnO. Since all the Zn-3d bands are fully occupied, no electron contribution is found at E_F. It is also observed that Zn-3p, 4s and O-2s states have an insignificant contribution to the total DOS (Figure 1 *c*).

Electronic properties of $Zn_{1-x}Cr_xO$ (x = 0.125, 0.25, 0.375, 0.5)

DOS calculations

The electronic properties of $Zn_{1-x}Cr_xO$ (x = 0.125, 0.25, 0.375, 0.5) were studied at RT structure. The first effort in this direction was the DOS calculations of $Zn_{1-x}Cr_xO$. The total DOS for x = 0.125, 0.25, 0.375 and 0.5 are shown in Figure 2. It is clear from this figure that ZnO encounters insulator to metal transition at 12.5% Cr doping. The spin majority species are metallic, whereas the minority spin species are insulating with a semiconducting gap ~2.5 eV (Figure 2 *a*). Further enhancement of Cr concentration dramatically changes the electrical conductivity of $Zn_{1-x}Cr_xO$. The system exhibits half-metal to metal transition at 25% Cr concentration (Figure 2 *b*). Nevertheless, an additional increase in Cr impurity within the crystal enhances TDOS at E_F and hence increases the electrical conductivity. The total DOS for x = 0.375 and 0.5 are also depicted in Figure 2 *c* and *d*.

The projected DOS of Zn-3d, Cr-3d and O-2p bands for x = 0.125, 0.25, 0.375 and 0.5 respectively, are presented in Figure 3 *a–d*. In all cases, the Zn-3d bands are found occupied in both spin channels and are pushed well below E_F. The calculated TDOS of Zn-3d bands at E_F remains almost 5 (states/eV/f.u./spin) in both spin channels (Table 2). From this table, it is also obvious that the number of Zn-3d electrons (n_{Zn}) for different values of x remains almost five in both spin channels which confirms that two electrons in each Zn-3d orbital are paired perfectly. It also emerges from the DOS calculations that the centre of gravity of the total DOS near E_F is predominantly due to Cr-3d character. The Cr-3d DOS for x = 0.125, 0.25, 0.375 and 0.5 are observed around –1.35 to 1.6 eV, –2.25 to –1.5 eV, –2.3 to 1.5 eV and –2.35 to 1.40 eV respectively, for the spin-up channel (Figure 3). The corresponding Cr-3d DOS for the down-spin channel are detected around 0.2 to 4.5 eV, –0.3 to 4.3 eV, –0.3 to 3.95 and –1.80 to 4.2 eV respectively. In addition, O-2*p* DOS for both spin channels are observed within –9.0 to 1.95 eV, –9.3 to –2.0 eV, –9.4 to –2.95 eV and –9.5 to –3.5 eV respectively, for x = 0.125, 0.25, 0.375 and 0.5 (Figure 3). It is clear from Table 2 that Cr-DOS reduces gradually in the spin majority channel, whereas increases sequentially with x for the spin minority channel. The doped systems $Zn_{1-x}Cr_xO$ are metallic in the spin majority channel. In the spin minority channel, all the Cr-3d-bands are almost unoccupied, but very tiny contributions of electrons were detected at E_F for $x \geq 0.25$. Therefore, the system is also metallic in this spin channel. Considering two spin channels, the system is therefore metallic for $x \geq 0.25$. Moreover, Zn-4*s*, 3*p*, Cr-3*p*, 3*s* and O-2*s* DOS are insignificant compared to the total DOS (not shown in figure).

Band structure calculations

To elucidate the origin of the insulator to half-metal (for x = 0.125) and then half-metal to metal (for $x \geq 0.25$) transition in $Zn_{1-x}Cr_xO$ precisely, electronic band structure calculations were also carried out for these systems. The partial band structure (PBS) of Cr-3d orbitals for the spin-up channel are shown in Figure 4 *a–l* respectively, for x = 0.125, 0.25, 0.375 and 0.5. The hexagonal crystal field splits Cr-3d bands into lower lying triply degenerate

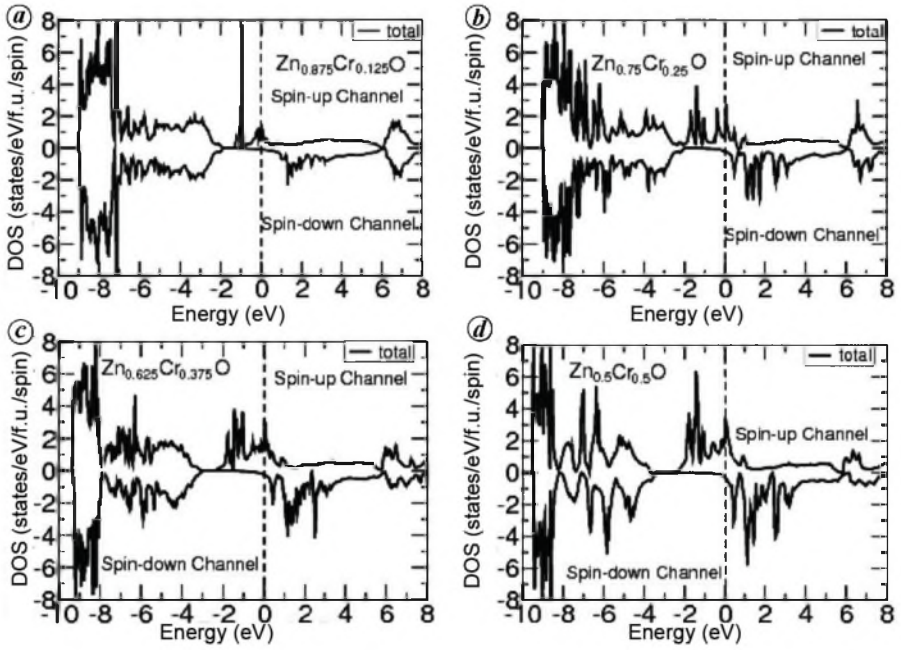

Figure 2. Calculated total DOS of $Zn_{1-x}Cr_xO$ for different doping levels. The doped system is half-metallic for $x = 0.125$ and metallic for all other cases. The Fermi energy is set to zero.

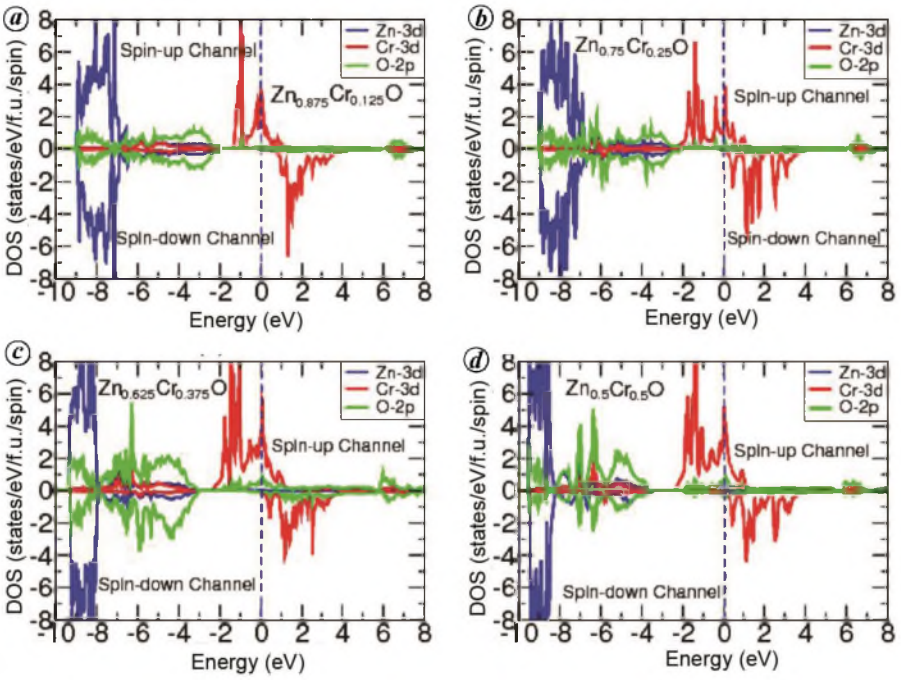

Figure 3. Calculated total Zn-3d (blue), Cr-3d (red) and O-2p (green) DOS of $Zn_{1-x}Cr_xO$ for different doping levels. The Fermi energy is set to zero.

t_{2g} and upper lying doubly degenerate e_g bands. The t_{2g} bands are further split into $d_{3z^2-r^2}$, d_{yz}, d_{xz} states and e_g bands into d_{xy} and $d_{x^2-y^2}$ states.

The PBS of Cr-3d states of $Zn_{0.875}Cr_{0.125}O$ for the spin majority channel is shown in Figure 4 *a–c*. It is observed from PBS calculations that the Cr-d_{yz} and d_{xz} orbitals are occupied by one electron each and are shifted below E_F (Figure 4 *b*). These states are observed to be exactly degenerate states. The Cr-$d_{3z^2-r^2}$ orbital is found partially filled (Figure 4 *c*) and touches E_F. The Cr-d_{xy} and $d_{z^2-r^2}$ orbitals are separated into bonding and anti-bonding components. The bonding components are observed occupied and are shifted below E_F, whereas the anti-bonding components are found unoccupied and are shifted above E_F (Figure 4 *a*). In the spin minority channel, all the Cr-3d orbitals are found unoccupied (not shown in the

Table 2. Calculated total densities of states (TDOS) at E_F and number of electrons of pure ZnO and $Zn_{1-x}Cr_xO$ (x = 0.125, 0.25, 0.375, 0.5) at 293 K

Compounds	Spin-up channel (↑)			Spin-down channel (↓)		
	Zn–3d	Cr–3d	O–2p	Zn–3d	Cr–3d	O–2p
DOS (states/eV/f.u./spin)						
ZnO	4.92	–	2.05	4.98	–	2.15
$Zn_{0.875}Cr_{0.125}O$	4.87	3.96	2.03	4.92	0	2.06
$Zn_{0.75}Cr_{0.25}O$	4.83	3.86	2.02	4.85	0.13	2.05
$Zn_{0.625}Cr_{0.375}O$	4.80	3.77	2.07	4.85	0.22	2.06
$Zn_{0.5}Cr_{0.5}O$	4.90	3.67	2.08	4.93	0.32	2.07
Number of electrons						
ZnO	4.91	–	2.04	4.90	–	2.04
$Zn_{0.875}Cr_{0.125}O$	4.90	3.95	2.04	4.90	0	2.04
$Zn_{0.75}Cr_{0.25}O$	4.90	3.88	2.03	4.90	0.10	2.03
$Zn_{0.625}Cr_{0.375}O$	4.90	3.77	2.03	4.90	0.20	2.03
$Zn_{0.5}Cr_{0.5}O$	4.90	3.69	2.07	4.90	0.30	2.03

figure). Therefore, $Zn_{0.875}Cr_{0.125}O$ is metallic in the spin majority channel due to electron contribution at E_F predominantly from the Cr-$d_{3z^2-r^2}$ orbital. Considering both spin channels, $Zn_{0.875}Cr_{0.125}O$ is thereby a half metal.

The next motivation was to optimize the PBS of $Zn_{0.75}Cr_{0.25}O$. The calculated Cr-3d PBS for the spin majority channel are displayed in Figure 4 *d–f*. It is visible from this figure that Cr-d_{yz} and d_{xz} orbitals are occupied by one electron each and they are exactly degenerate (Figure 4 *e*). These orbitals are pushed well below the Fermi level. The $d_{3z^2-r^2}$ orbital is partially occupied and still touches E_F (Figure 4 *f*). The occupancy of this orbital increases slightly compared to the corresponding orbital of $Zn_{0.875}Cr_{0.125}O$. The two e_g orbitals (d_{xy} and $d_{x^2-y^2}$) are also found to have occupied bonding components and unoccupied anti-bonding components (Figure 4 *d*). These two orbitals remain degenerate, but their bonding components touch E_F. Therefore, the leading electron contribution at E_F from the partially occupied Cr-$d_{3z^2-r^2}$ orbital is principally responsible for the metallic behaviour of $Zn_{0.875}Cr_{0.125}O$ in the spin majority channel. Nevertheless, the scenario changes dramatically in the spin minority channel. Finite but small contributions of electrons at E_F were observed from d_{xy} and $d_{x^2-y^2}$ orbitals. These two orbitals were found exactly degenerate (Figure 4 *m*) and just touch E_F. Consequently, the material $Zn_{0.75}Cr_{0.25}O$ is a metal. Further, the PBS of Cr-$d_{yz/xz}$, $d_{3z^2-r^2}$ and d_{xy}/x^2-y^2 orbitals for the spin majority channel of $Zn_{0.625}Cr_{0.375}O$ and $Zn_{0.5}Cr_{0.5}O$ are also shown in Figure 4 *g–l*. The trend remains the same as that observed for $Zn_{0.75}Cr_{0.25}O$. The only difference is that the occupancies of $d_{3z^2-r^2}$ orbitals increase slightly, whereas decrease for d_{xy}/x^2-y^2 orbitals for the spin majority channel. Besides this, both systems are observed metallic in the down-spin channels due to minute contributions of electrons at E_F from the d_{xy}/x^2-y^2 orbitals. Nevertheless, the occupancies of these states are in increasing order compared to those orbitals of $Zn_{0.75}Cr_{0.25}$. Therefore, these two compounds $Zn_{0.625}Cr_{0.375}O$ and $Zn_{0.5}Cr_{0.5}O$ are also metallic.

To be clear of the underlying physics behind the insulator to half-metal and then half-metal to metal transition of Cr-doped ZnO for different doping levels, the total ground state energies (E_T), TDOS and number of electrons are also calculated. It is obvious from Table 1 that E_T decreases drastically with increase in x. This result indicates that the electron correlation effect increases rapidly due to increase in Cr concentration. The spin polarization calculated for x = 0.125, 0.25, 0.375 and 0.5 are 100%, 80%, 75% and 66% respectively. Therefore, 100% spin polarization accompanied by strong dynamical electron correlation is responsible for the half-metallic behaviour of $Zn_{0.875}Cr_{0.125}O$. Nevertheless, the spin polarization of $Zn_{0.75}Cr_{0.25}$, $Zn_{0.625}Cr_{0.375}O$ and $Zn_{0.5}Cr_{0.5}O$ are high enough compared to normal metals for which spin polarization is only 36–47%. It is evident from Table 2 that the number of Cr-3d electrons (n_{Cr}) for the spin majority channel decreases slowly, while n_{Cr} increases gradually for the spin minority channel with increasing Cr impurities. Therefore, the addition of Cr increases the electrical conductivity by adding free electron into the minority spin channel near E_F due to high spin polarizations arising from strong dynamical electron correlation.

Magnetic properties of ZnO and $Zn_{1-x}Cr_xO$ (x = 0.125, 0.25. 0.375, 0.5)

In this section, the magnetic properties of $Zn_{1-x}Cr_xO$ have been studied extensively. The formal valence of Cr in all $Zn_{1-x}Cr_xO$ (x = 0.125, 0.25, 0.375, 0.5) compounds is +2 (Cr^{2+}), i.e. the number of d electron is 4 (d^4). Further, it is evident from DOS calculations that electrons in the Zn-3d orbitals are perfectly paired in opposite spin direction resulting in zero net magnetic moments. Consequently,

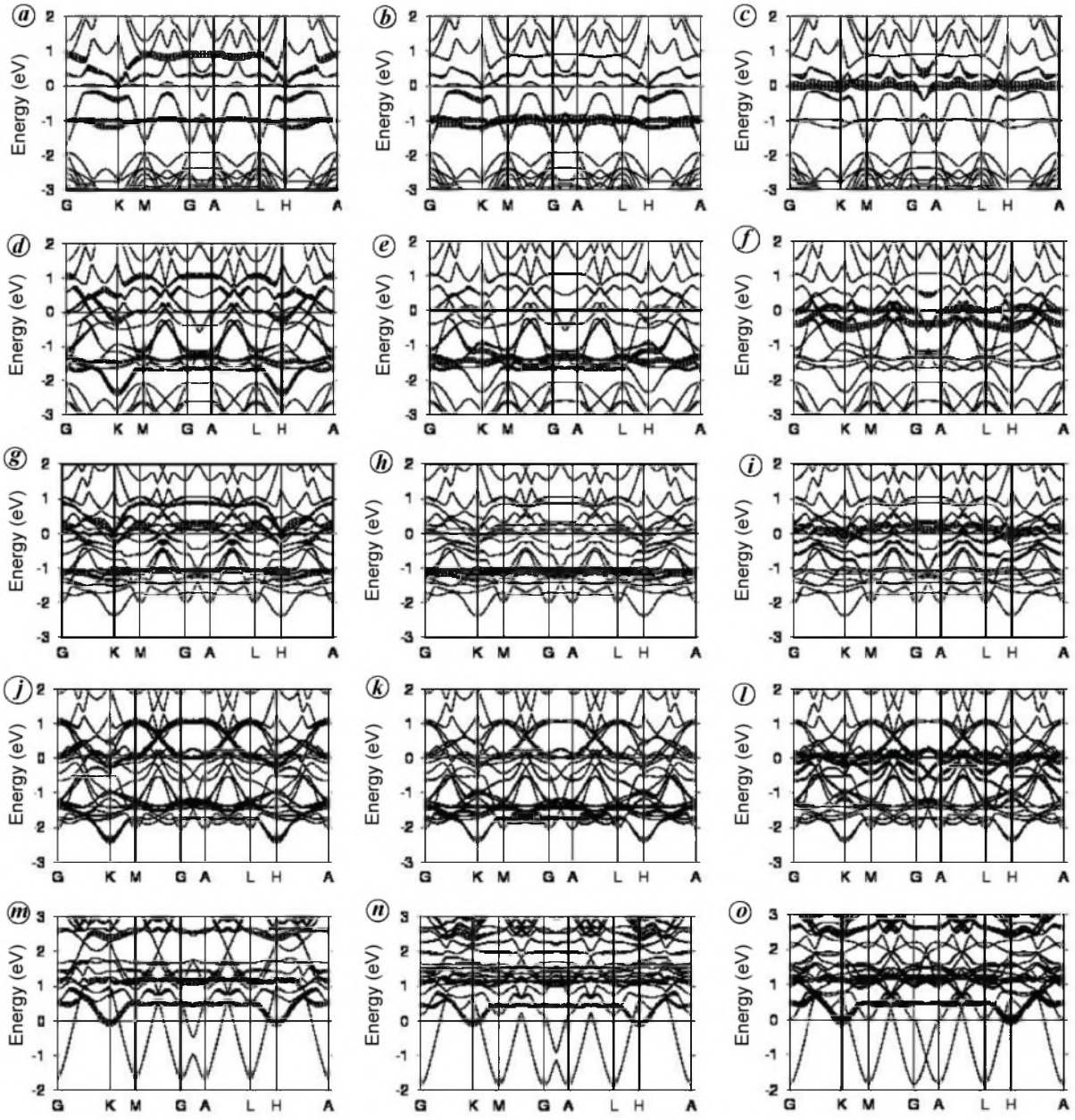

Figure 4. Calculated partial band structure (PBS) of different orbitals of Cr in doped ZnO. In the spin-up channel, the PBS of Cr-d_{xy/x^2-y^2}, $d_{yz/xz}$ and $d_{3z^2-r^2}$ orbitals are represented respectively, by (***a***, ***b***, ***c***) $Zn_{0.875}Cr_{0.125}O$, (***d***, ***e***, ***f***) $Zn_{0.725}Cr_{0.25}O$, (***g***, ***h***, ***i***) $Zn_{0.625}Cr_{0.375}O$ and (***j***, ***k***, ***l***) $Zn_{0.5}Cr_{0.5}O$. The PBS of Cr-d_{xy/x^2-y^2} orbitals for the spin-down channel are represented in ***m***, ***n*** and ***o*** for $Zn_{0.725}Cr_{0.25}O$, $Zn_{0.625}Cr_{0.375}O$ and $Zn_{0.5}Cr_{0.5}O$ respectively.

pure ZnO is a non-magnetic insulator. Since the net magnetic moments arises from Zn is zero for all $Zn_{1-x}Cr_xO$ materials, the magnetism of these compounds is primarily determined by the orientations of Cr-spins. For $Zn_{0.875}Cr_{0.125}O$, it is obvious from the n_{Cr} and DOS calculations (Tables 1 and 2) that all the four Cr-3d electrons are distributed in the spin-up channel. These electrons are further oriented in the parallel direction and thereby are coupled ferromagnetically, that results in net Cr-magnetic moments (μ_{Cr}) = –3.97 μ_B. The FM in this compound arises from strong Hund's rule coupling between electrons in the Cr-3d orbitals. For $Zn_{0.75}Cr_{0.25}O$, the number of up-spin electrons is 3.88 whereas the number of down-spin electrons is 0.10 resulting in μ_{Cr} = 3.8 μ_B. As a result, Hund's rule coupling is responsible for the ferromagnetism in $Zn_{0.75}Cr_{0.25}O$. The number of up and down spin electrons of $Zn_{0.625}Cr_{0.375}O$ (or $Zn_{0.5}Cr_{0.5}O$) is 3.77 and 0.2 (or 3.69 and 0.30) respectively (Table 2). Subsequently, the net Cr magnetic moments for these two materials are 3.6 and 3.4 μ_B respectively (Table 1). Consequently, $Zn_{0.625}Cr_{0.375}O$ and $Zn_{0.5}Cr_{0.5}O$ are also FM. Eventually, it is merely observed in this study that the strength of FM decreases with the augmentation of Cr-concentration. In addition, it is clear from Table 1 that

Table 3. Calculated bond lengths and bond angles of pure ZnO and $Zn_{0.5}Cr_{0.5}O$ in the hexagonal wurtzite structure at 293 K

	ZnO		$Zn_{0.5}Cr_{0.5}O$	
	Basal	Apical	Basal	Apical
Bond lengths (Å)				
Zn–O	1.9746 × 3	1.9857	1.9824 × 3	1.9564
Cr–O	–	–	1.9824 × 3	1.9564
Zn–Zn	3.2080	3.2489	3.2066	3.2467
Cr–Cr	–	–	3.2066	3.2467
Bond angles (°)				
∠Zn–O–Zn	110.70 × 3	108.202	109.945 × 3	108.993
∠Cr–O–Cr	–	–	109.945 × 3	108.993

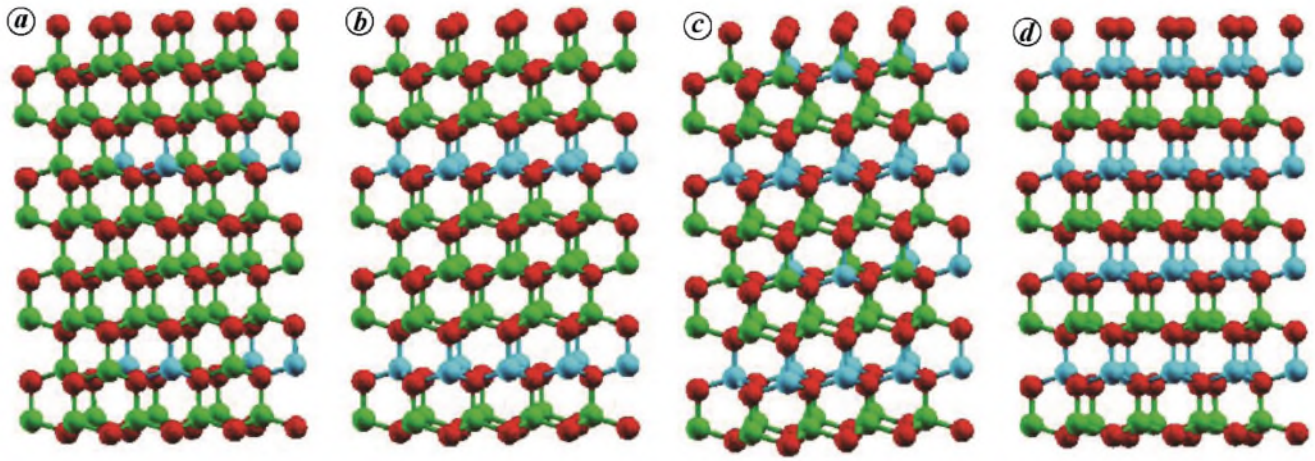

Figure 5. Crystal structures of (***a***) pure ZnO and (***b***) $Zn_{0.5}Cr_{0.5}O$. The Zn, O and Cr atoms are represented by green, red and cyan spheres.

the Zn-magnetic moments remain almost zero (–0.01 μ_B) throughout the subtitution process. The O-magnetic moments increase gradually with increasing Cr content. Interestingly, all O-ions are ferromagnetically coupled with Cr-ions. It is also observed from the PBS calculations that the available four Cr electrons are distributed in all the 3d orbitals due to strong Hund's rule coupling. Further, small but gradual increase in the number of down spins for $x \geq 0.25$ is observed due to increase in the Hund's rule coupling, which is also reflected in the E_T calculations for the doped compounds. It is observable from Table 1 that E_T increases significantly due to Cr doping in ZnO. Thus the repulsive force increases with Cr impurities, indicating increase in electron correlations. Therefore, Hund's rule coupling is responsible for this augmentation of electron correlations. Therefore, the Cr-3d electrons align ferromagnetically due to strong electron correlations accompanied by strong Hund's rule coupling.

Structural properties of ZnO and $Zn_{1-x}Cr_xO$ ($x = 0.5$)

Structures of pure ZnO in the RT wurtzite structure are presented in Figure 1 *d*. The primitive unit cell of pure ZnO consists of two Zn and O atoms each. Each Zn atom has four-fold coordinations with O atoms. These four O atoms form the regular ZnO_4 tetrahedron with Zn at the centre. In each ZnO_4 tetrahedron, there is a single apical O atom (in the *c*-direction) and three basal O atoms (in the *ab* plane). The Zn–O/Zn–Zn bond distances and ∠Zn–O–Zn bond angles are reported in Table 3.

Next, concentration has been paid for the crystal structure of $Zn_{1-x}Cr_xO$ for $x = 0.125$, 0.25, 0.375 and 0.5 respectively are shown in Figure 5 *a–d*. In these doped materials, two types of oxygen coordination are detected in the *c*-direction causing the formation of ZnO_4 and CrO_4 tetrahedrons. However, the bond distances and bond angles remain almost identical up to $x = 0.375$. Nevertheless, only a minute change in the structure is observed for $x = 0.5$. All the Zn–O, Cr–O, Zn–Zn and Cr–Cr bond lengths and ∠Zn–O–Zn and ∠Cr–O–Cr bond angles of $Zn_{0.5}Cr_{0.5}O$ are given in Table 3. It is evident from this table that the apical Zn–O bonds lengths reduce by 0.0293 Å, while the basal Zn–O bond lengths enhance by 0.0078 Å. Furthermore, both Zn–Zn apical and basal bonds distances shorten by 0.0022 and 0.0014 Å respectively. All the ∠Zn–O–Zn and ∠Cr–O–Cr bond angles in the basal plane are equal (109.945°). The ∠Zn–O–Zn bond angle in the apical plane is increased by 0.791° and

decreased by 0.755° in the basal plane. Therefore, Cr-doping in pure ZnO invokes a very small structural distortion which is hard to detect experimentally.

Conclusion

In summary, it is observed that pure ZnO is a nonmagnetic insulator with a band gap 1.9 eV. It is found in this study that each of Zn–3d orbital is occupied by two electrons which are further paired in opposite direction and responsible for the nonmagnetic insulating behaviour of ZnO at RT. But the scenario changes significantly for Cr doping. This material encounters nonmagnetic insulator to a ferromagnetic half-metal (FHM) and then FHM to a ferromagnetic metal for $x = 0.15$ and 0.25 respectively. The FM metallic phase is found to maintain up to $x = 0.5$. It is revealed that 100% spin polarization is responsible for the half-metallic behaviour of $Zn_{0.875}Cr_{0.125}O$. Nevertheless, small but finite electron contributions from the Cr-d_{xy/x^2-y^2} orbitals at E_F for the spin-down channel causes the metallic behaviour of $Zn_{1-x}Cr_xO$ ($x \geq 0.25$). All the doped materials exhibit ferromagnetism arising from strong Hund's rule coupling. However, a small variation in the Zn–O/Zn–Zn bond distances and ∠Zn–O–Zn bond angles caused by Cr doping is responsible for little structural distortions in $Zn_{1-x}Cr_xO$.

1. Yoshio, K., Onodera, A., Satoh, H., Sakagami, N. and Yamashitam, H., Crystal structure of ZnO : Li at 293 K and 19 K by X-ray diffraction. *Ferroelectrics*, 2001, **264**, 133–138.
2. Look, D. C., Recent advances in ZnO materials and devices. *Mater. Sci. Eng. B*, 2001, **80**, 383.
3. Wei, Z. P. *et al.*, Room temperature *p–n* ZnO blue–violet light-emitting diodes. *Appl. Phys. Lett.*, 2007, **90**, 042113.
4. Mandalapu, L. J., Yang, Z., Chu, S. and Liu, J. L., Ultraviolet emission from Sb-doped *p*-type ZnO based heterojunction light-emitting diodes. *Appl. Phys. Lett.*, 2008, **92**, 122101.
5. Lee, J., Lee, H., Seo, S. and Park, J., Characterization of undoped and Cu-doped ZnO films for surface acoustic wave applications. *Thin Solid Films*, 2001, **398**, 641.
6. Chen, H. Y., Bagnall, D. and Yao, T., ZnO as a novel photonic material for the UV region. *Mater. Sci. Eng. B*, 2000, **75**, 190.
7. Liang, S., Sheng, H., Liu, Z., Hio, Z., Lu, Y. and Shen, H., ZnO Schottky ultraviolet photodetectors. *J. Cryst. Growth*, 2001, **225**, 110–113.
8. Lee, J. Y., Choi, Y. S., Kim, J. H., Park, O. and Im, S., Optimizing *n*-ZnO/*p*-Si heterojunctions for photodiode applications. *Thin Solid Films*, 2002, **403**, 553–537.
9. Golego, N., Studenikin, S. A. and Cocivera, M., Sensor photoresponse of thin film oxides of zinc and titanium to oxygen gas. *J. Electrochem. Soc.*, 2000, **147**, 1592–1594.
10. Djurisic, A. B., Ng, A. M. C. and Chen, X. Y., ZnO nanostructures for optoelectronics: Material properties and device applications. *Prog. Quant. Electron.*, 2010, **34**, 191–259.
11. Al-Kahlout, A., ZnO nanoparticles and porous coatings for dye-sensitized solar cell application: photoelectrochemical characterization. *Thin Solid Films*, 2012, **520**, 1814–1820.
12. Li, P., Wang, S., Li, J. and Wei, Y., Structural and optical properties of Co-doped ZnO nanocrystallites prepared by a one-step solution route. *J. Lumin.*, 2012, **132**, 220–225.
13. Huang, Y., Zhang, Y., Gu, Y., Bai, X., Qi, J., Liao, Q. and Liu, J. Field emission of a single in-doped ZnO nanowire. *J. Phys. Chem. C. Nanometer. Interf.*, 2012, **111**, 9039–9043.
14. Venkatesan, M., Fitzgerald, C. B., Lunney, J. G. and Coey, J. M. D., Anisotropic ferromagnetism in substituted zinc oxide. *Phys. Rev. Lett.*, 2004, **93**, 177206.
15. Jin, Z. *et al.*, High throughput fabrication of transition-metal-doped epitaxial ZnO thin films: a series of oxide-diluted magnetic semiconductors and their properties. *Appl. Phys. Lett.*, 2001, **78**, 3824.
16. Liu, H. *et al.*, Role of point defects in room-temperature ferromagnetism of Cr-doped ZnO. *Appl. Phys. Lett.*, 2007, **91**, 072511.
17. Hohenberg, P. and Kohn, W., Inhomogeneous electron gas. *Phys. Rev. B*, 1964, **136**, B864.
18. Kohn, W. and Sham, L. J., Self-consistent equations including exchange and correlation effects. *Phys. Rev.*, 1965, **140**, A1133.
19. Perdew, J. P. and Wang, Y., Accurate and simple analytic representation of the electron gas correlation energy. *Phys. Rev. B Condens. Matter. Mater. Phys.*, 1992, **45**, 13244.
20. Anderson, O. K. and Jepsen, O., Explicit, first-principles tight-binding theory. *Phys. Rev. Lett.*, 1984, **53**, 2571.
21. Anderson, O. K., Linear methods in band theory. *Phys. Rev. B Condens. Matter. Mater. Phys.*, 1975, **12**, 3060.
22. Xie, F. W., Yang, P., Li and Zhang, L. Q., First-principle study of optical properties of (N, Ga) codoped ZnO. *Opt. Commun.*, 2012, **285**, 2660–2664.

Received 2 September 2017; revised accepted 30 July 2018

doi: 10.18520/cs/v115/i8/1504-1511